Electronic Supplementary Material (ESI) for RSC Advances

Electronic Supplementary Information

Design and evaluation of nano-biphasic ionic liquid systems having highly polar and low polar domains

Satomi Taguchi, Takahiro Ichikawa, Takashi Kato, and Hiroyuki Ohno*

Selection of dye molecules for polarity measurements

We have checked that these dyes shown below were not suitable for the evaluation of polarity in the present nano-biphasic IL system because these dyes were soluble in both IL (**1** and **2**). As seen in Fig. S1, dyes (a, b, and c) seem to be useful to analyse only upper IL phase, they were detected by spectroscopic measurements.

Fig. S1 Structure of hydrophobic ionic liquid (IL) **1** and hydrophilic IL**2**. Photograph of the macro-segregated IL system composed of **1** and **2** containing various dyes: (a) 5-bromo-5"-formyl-2,3":5',2"-terthiophene, (b) Nile red(c) rhodamine 6G, (d) rhodamine B, (e) coumarine 153 (f) Indoine blue and (g) indigo.

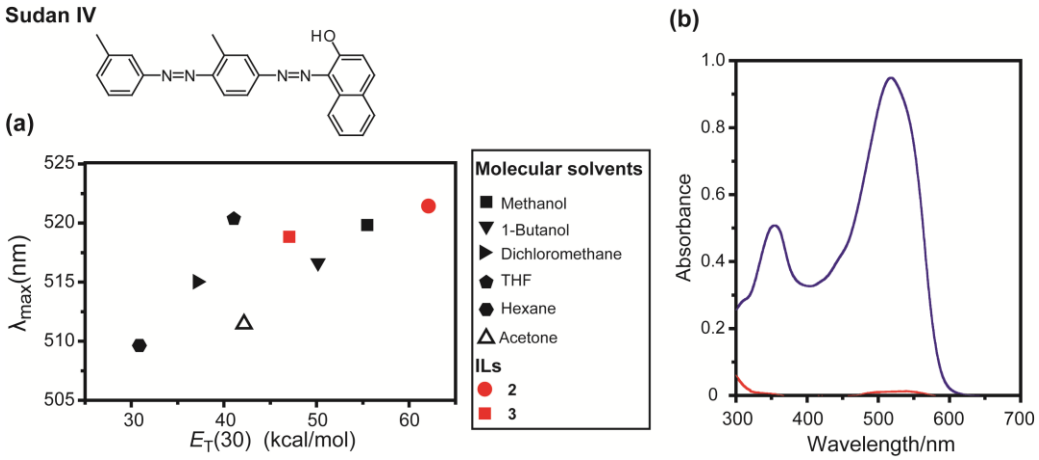

Fig. S2 (a) Comparison of the value of $E_T(30)$ in some conventional molecular solvents and ILs and the absorption peak of Sudan IV observed at around 510 nm (λ_{max}). (b) UV-vis absorption Spectra of sudan IV in hydrophilic IL phase (red line) and hydrophobic IL phase (blue line) of the macro-separated IL system.

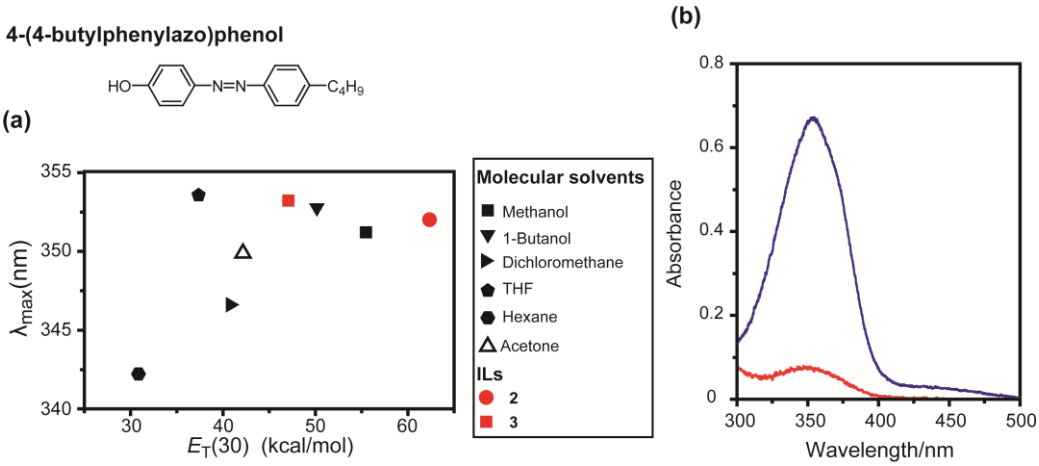

Fig. S3 (a) Comparison of the value of $E_T(30)$ in some conventional molecular solvents and ILs and the absorption peak of 4-(4-buthylphenylazo)phenol at around 350 nm (λ_{max}). (b) UV-vis absorption spectra of 4-(4-buthylphenylazo)phenol in hydrophilic IL phase (red line) and hydrophobic IL phase (blue line) of the macro-separated IL system.

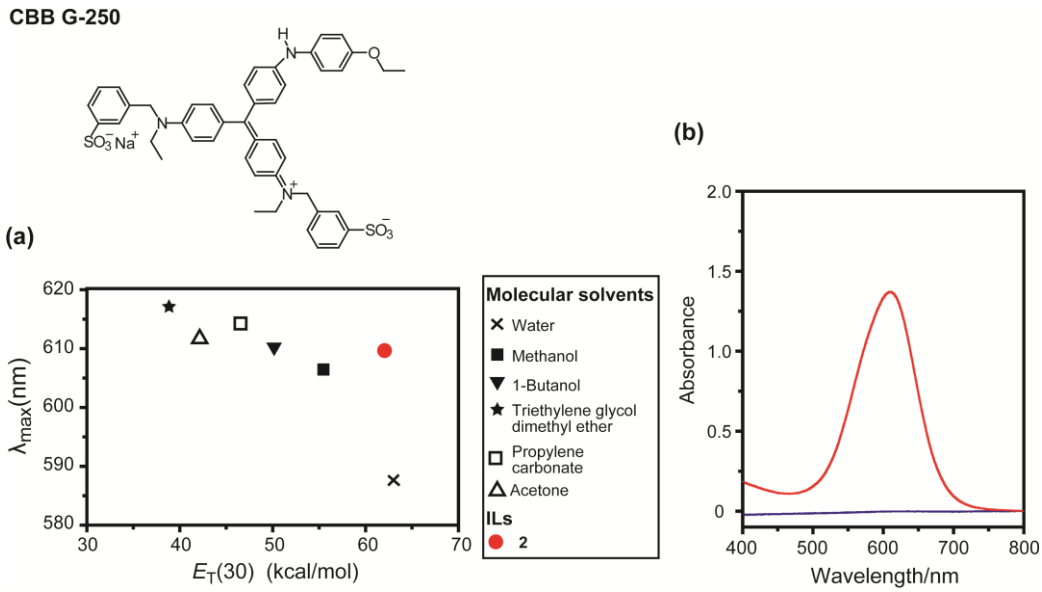

Fig. S4 (a) Comparison of the value of $E_T(30)$ in some conventional molecular solvents and IL**2** and the absorption peak of CBB G-250 at around 600 nm (λ_{max}). (b) UV-vis absorption spectra of CBB G-250 in hydrophilic IL phase (red line) and hydrophobic IL phase (blue line) of the macro-separated IL system.

Phase diagram of the IL 2 and 3 mixture

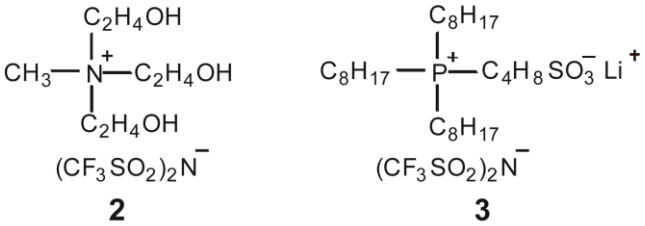

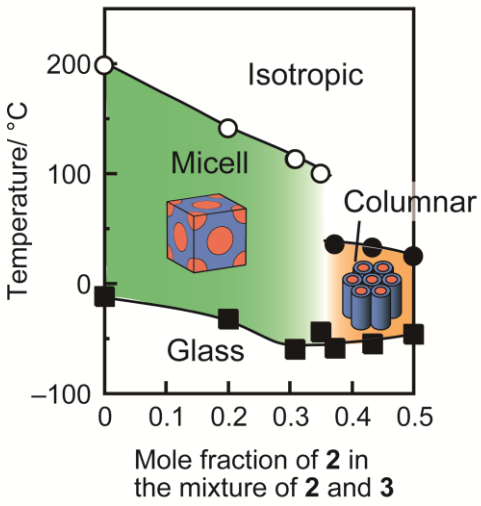

Fig. S5 Phase diagram of the mixture of **2** and **3**.

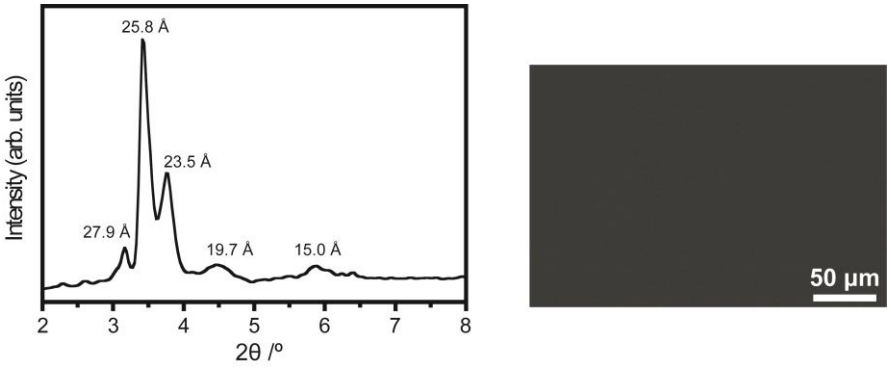

Fig. S6 Small-angle X-ray scattering pattern and polarising optical micrograph of **2**/**3** mixture (mole fraction 0.35 for **2**) at 60 °C.

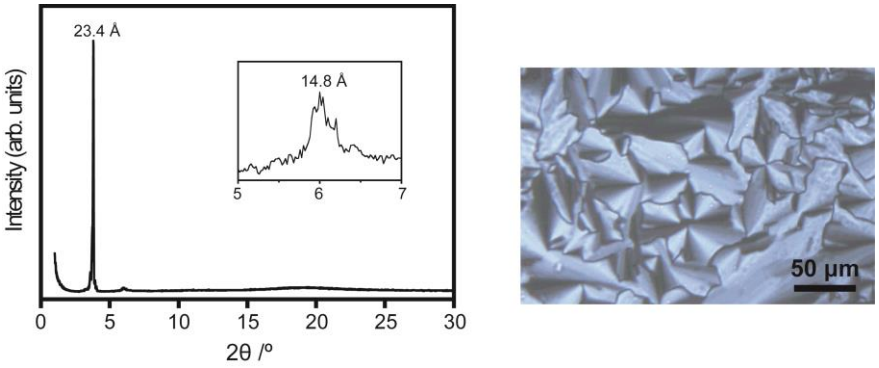

Fig. S7 Wide-angle X-ray diffraction pattern and polarising optical micrograph of **2**/**3** mixture (mole fraction 0.5 for **2**) at 30 °C.

Nano-segregated structures of **2**/**3** mixtures were confirmed by X-ray measurement and polarising optical microscopic observation. The small-angle X-ray scattering pattern of **2**/**3** mixture (mole fraction 0.35 for **2**) at 60 °C shows five peaks (Fig. S6). On the other hand, the X-ray pattern of **2**/**3** mixture (mole fraction 0.5 for **2**) shows a considerably different X-ray pattern from that of **2**/**3** mixture (mole fraction 0.35 for **2**). For example, the wide angle X-ray diffraction pattern of **2**/**3** mixture (mole fraction 0.5 for **2**) at 30 °C shows one intense peak at 3.78° (23.4 Å) and one weak peak at 5.98° (14.8Å) (Fig. S7). The reciprocal *d*-spacing ratio of the two peaks is 1 : √3, which can be assigned to the (100) and (110) reflections of a hexagonal columnar structure with the *p6mm* symmetry. Polarising optical microscopic observation for **2**/**3** mixture (mole fraction 0.5 for **2**) further supports the formation of the columnar structure.